P13.1

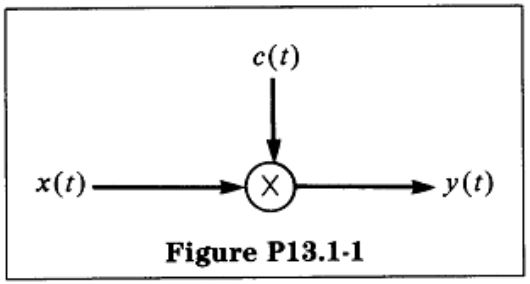

Figure P13.1-1

In the amplitude modulation system in Figure P13.1-1, the input $x(t)$ has the Fourier transform shown in Figure P13.1-2.

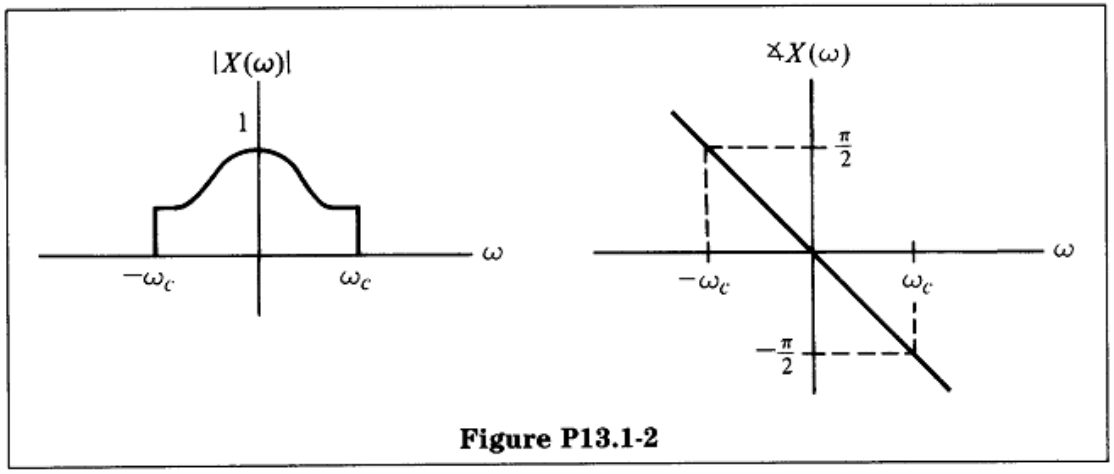

Figure P13.1-2

For each choice of carrier $c(t)$ in the following list, draw the magnitude and phase of $Y(\omega)$, the Fourier transform of $y(t)$.

[redacted]

(c) $c(t) = \cos 3\omega_c t$

(d) $c(t) = \sin 3\omega_c t$

[redacted]

c)

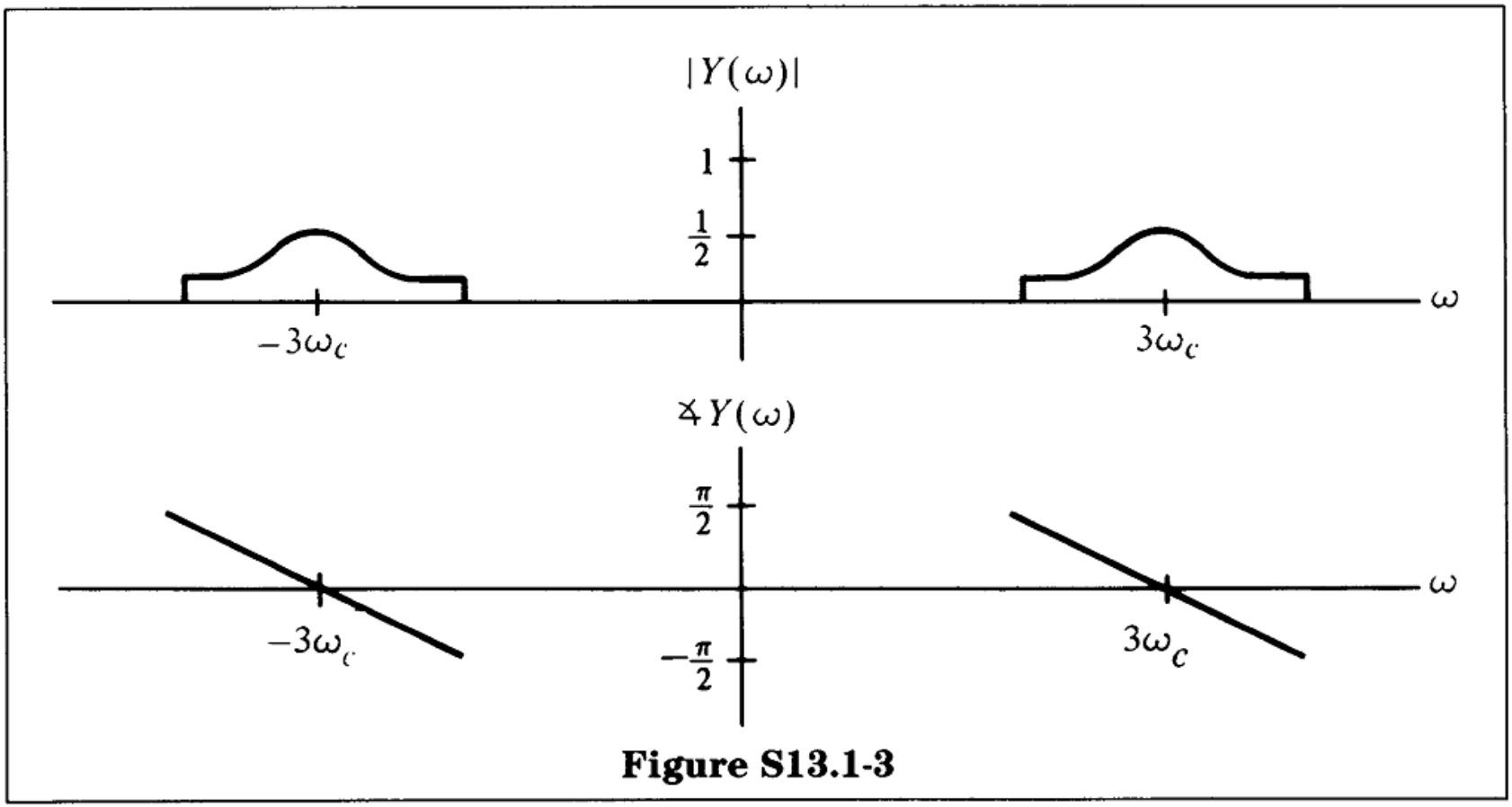

Figure S13.1-3

d)

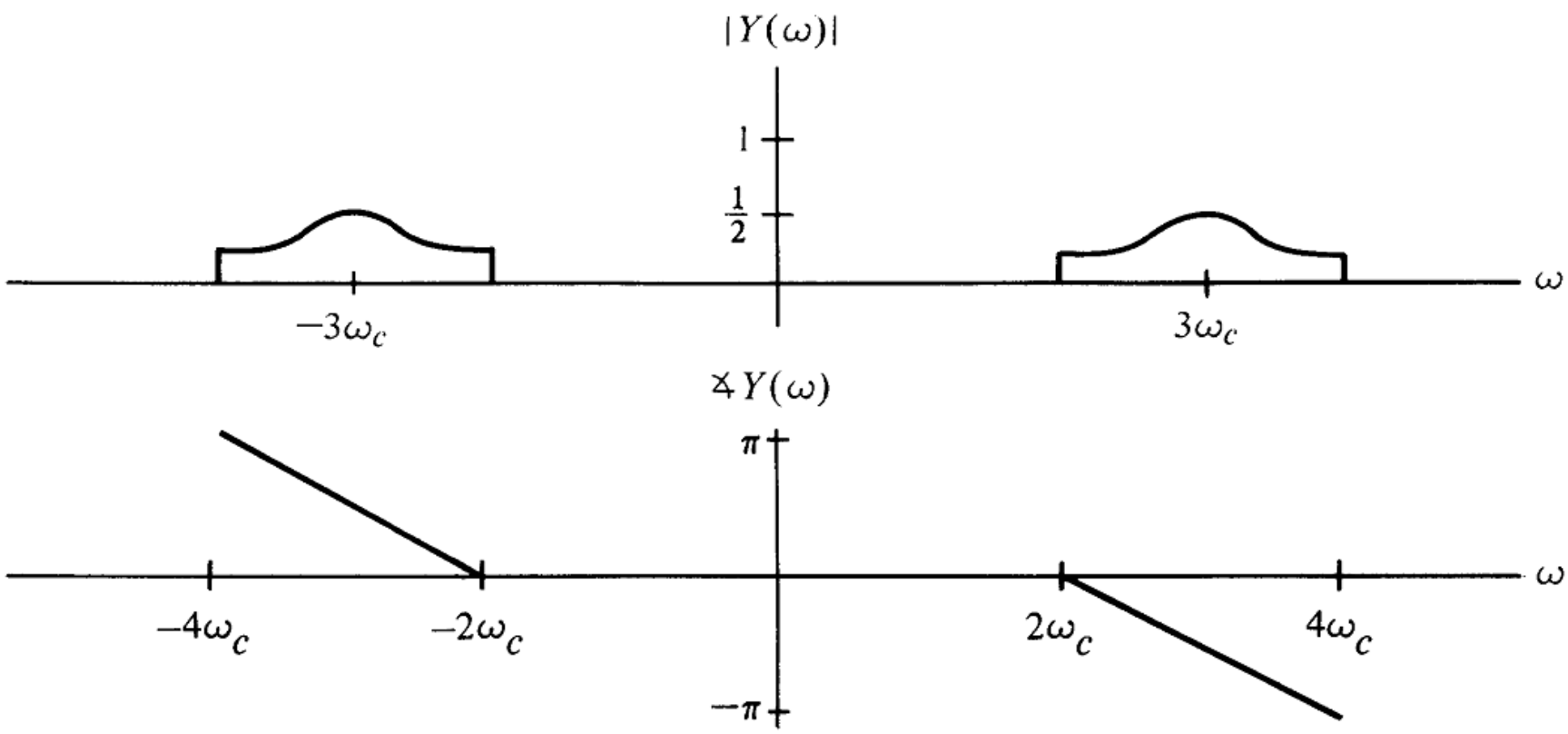

Figure S13.1-4

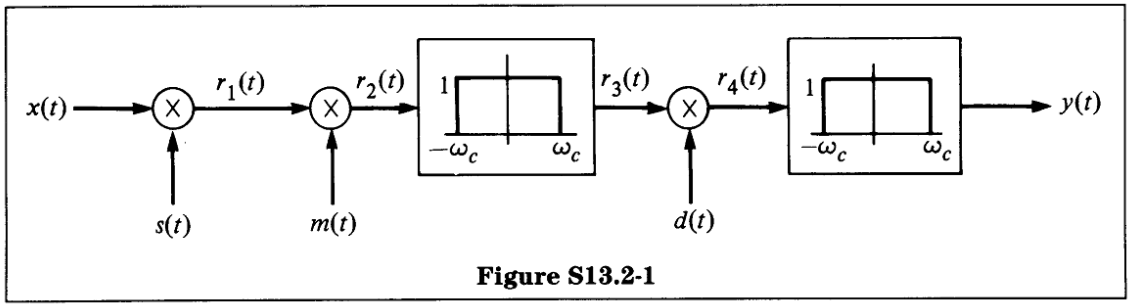

Figure S13.2-1

The Fourier transform of $s(t)$ is given by Figure P13.2-2.

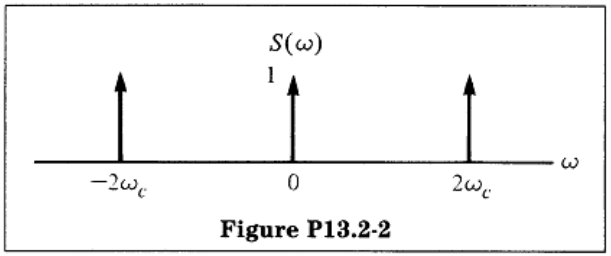

Figure P13.2-2

The Fourier transform of $x(t)$ is given by Figure P13.2-3.

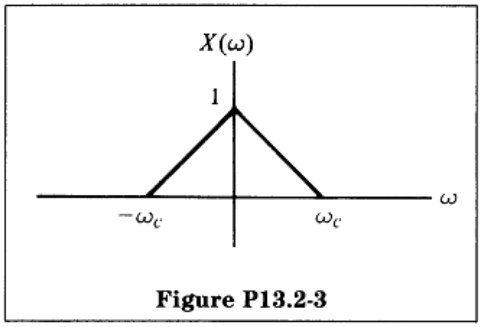

Figure P13.2-3

For which of the following choices for $m(t)$ and $d(t)$ is $y(t)$ nonzero?

	$m(t)$	$d(t)$
(a)	1	1
(b)	$\cos \omega_c t$	$\cos \omega_c t$

By the modulation property, $R_1(\omega)$, the Fourier transform of $r_1(t)$, is

$$R_1(\omega) = \frac{1}{2\pi}[X(\omega) * S(\omega)]$$

Since $S(\omega)$ is composed of impulses, $R_1(\omega)$ is a repetition of $X(\omega)$ centered at $-2\omega_c$, 0, and $2\omega_c$, and scaled by $1/(2\pi)$. See Figure S13.2-2.

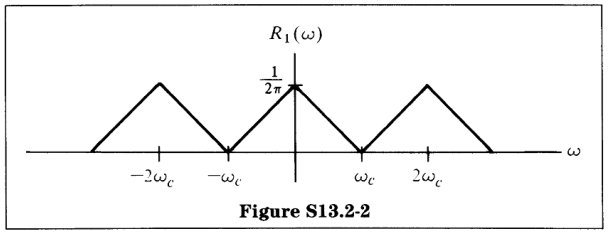

Figure S13.2-2

(a) Since $m(t) = d(t) = 1$, $y(t)$ is $r_1(t)$ filtered twice by the same ideal lowpass filte with cutoff at ω_c. Thus, comparing the resulting Fourier transform of $y(t)$ shown in Figure S13.2-3, we see that $y(t) = 1/(2\pi)x(t)$, which is nonzero.

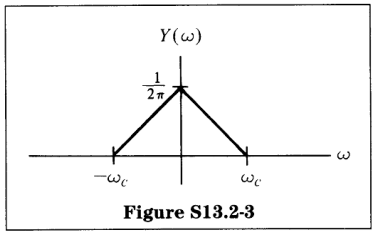

Figure S13.2-3

b)

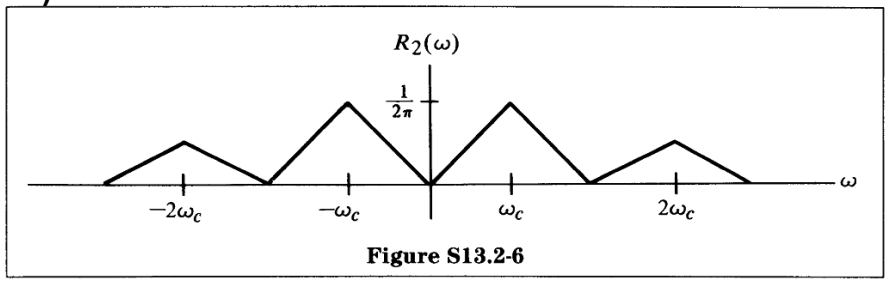

Figure S13.2-6

After filtering, $R_3(\omega)$ is given as in Figure S13.2-7.

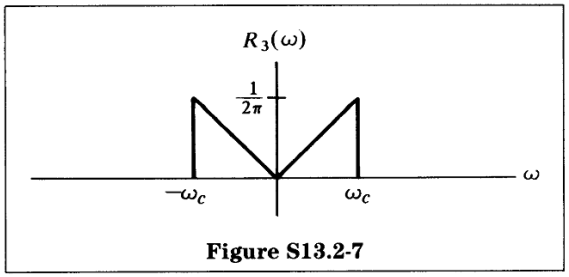

Figure S13.2-7

$R_4(\omega)$ is given by shifting $R_3(\omega)$ up and down by ω_c and dividing by 2. See Figure S13.2-8.

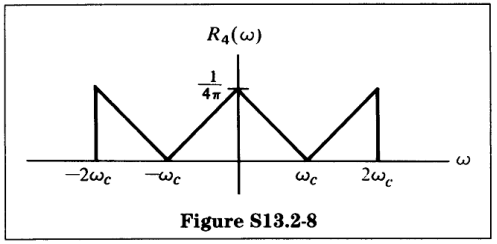

Figure S13.2-8

After filtering, $Y(\omega)$ is as shown in Figure S13.2-9.

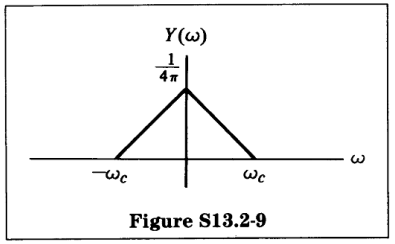

Figure S13.2-9

Comparing $Y(\omega)$ and $X(\omega)$ yields

$$y(t) = \frac{1}{4\pi}x(t)$$

P13.8

A commonly used system to maintain privacy in voice communications is a speech scrambler. As illustrated in Figure P13.8-1, the input to the system is a normal speech signal $x(t)$ and the output is the scrambled version $y(t)$. The signal $y(t)$ is transmitted and then unscrambled at the receiver.

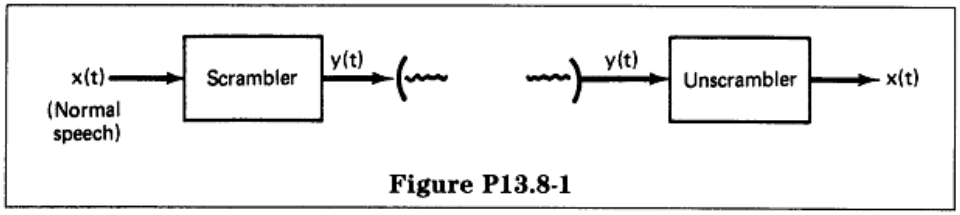

Figure P13.8-1

We assume that all inputs to the scrambler are real and bandlimited to frequency ω_M; that is, $X(\omega) = 0$ for $|\omega| > \omega_M$. Given any such input, our proposed scrambler permutes different bands of the input signal spectrum. In addition, the output signal is real and bandlimited to the same frequency band; that is, $Y(\omega) = 0$ for $|\omega| > \omega_M$. The specific permuting algorithm for our scrambler is

$$Y(\omega) = X(\omega - \omega_M), \qquad 0 < \omega < \omega_M,$$
$$Y(\omega) = X(\omega + \omega_M), \qquad -\omega_M < \omega < 0$$

(a) If $X(\omega)$ is given by the spectrum shown in Figure P13.8-2, sketch the spectrum of the scrambled signal $y(t)$.

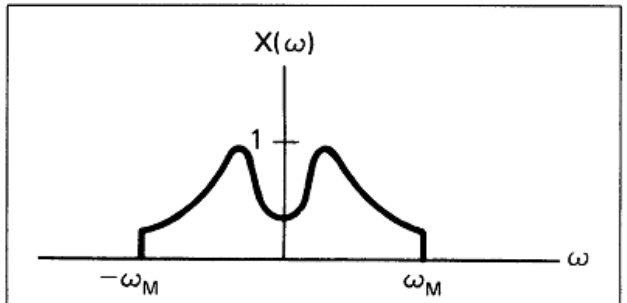

Figure P13.8-2

(b) Using amplifiers, multipliers, adders, oscillators, and whatever ideal filters you find necessary, draw the block diagram for such an ideal scrambler.

(c) Again, using amplifiers, multipliers, adders, oscillators, and ideal filters, draw a block diagram for the associated unscrambler.

(a) $X(\omega)$ is given as in Figure S13.8-1.

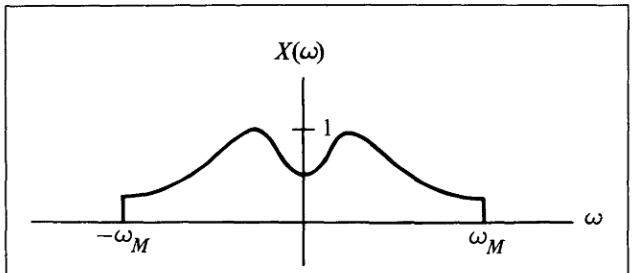

Figure S13.8-1

For $Y(\omega)$, the spectrum of the scrambled signal is as shown in Figur

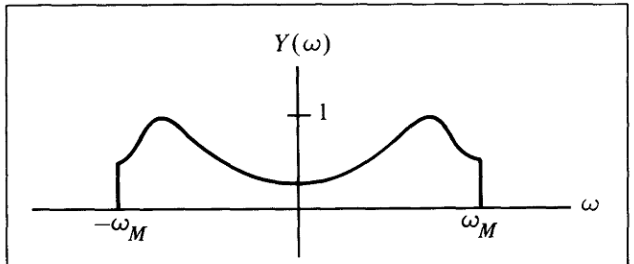

Figure S13.8-2

Thus, $X(\omega)$ is reversed for $\omega > 0$ and $\omega < 0$.

(b) Suppose we multiply $x(t)$ by $\cos \omega_M t$. Denoting $z(t) = x(t)\cos \omega_M t$, we find that $Z(\omega)$ is composed of scaled versions of $X(\omega)$ centered at $\pm\omega_M$. See Figure S13.8-3.

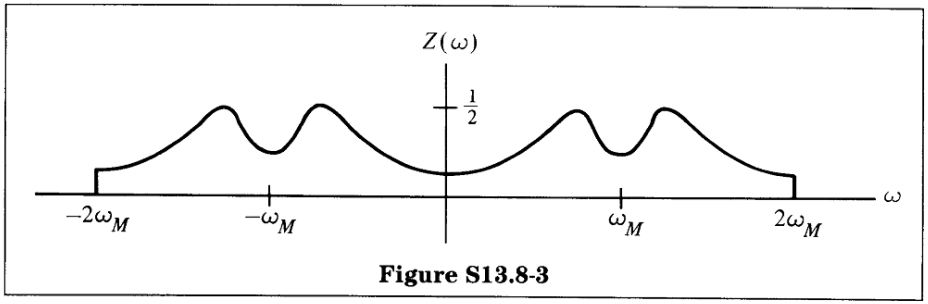

Figure S13.8-3

Filtering $z(t)$ with an ideal lowpass filter with a gain of 2 yields $y(t)$, as shown in Figure S13.8-4.

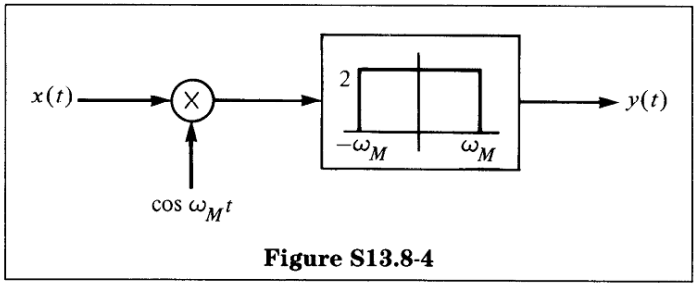

Figure S13.8-4

(c) Suppose we use the same system to recover $x(t)$. Let $y(t)\cos \omega_M t = r(t)$. Then $R(\omega)$ is as given in Figure S13.8-5.

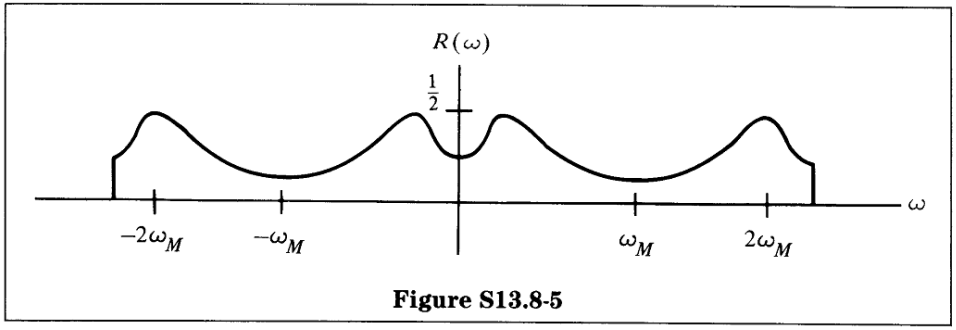

Figure S13.8-5

Filtering with the same lowpass filter yields $x(t)$.

For each of the time waveforms (a)–(j) (Figures P14.3-1 to P14.3-10), match its possible spectrum (i)–(x) (Figures P14.3-11 to P14.3-20).

(a)

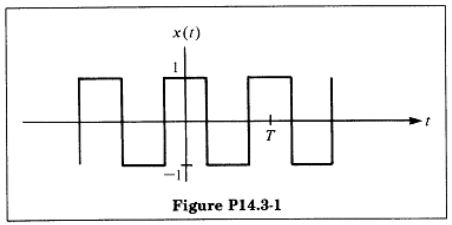

Figure P14.3-1

(b)

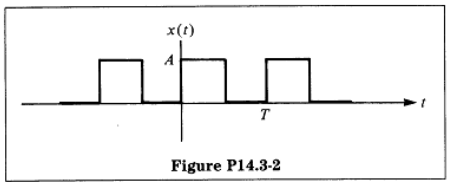

Figure P14.3-2

(c)

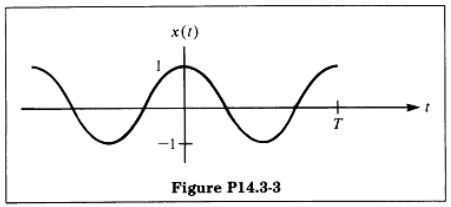

Figure P14.3-3

(d)

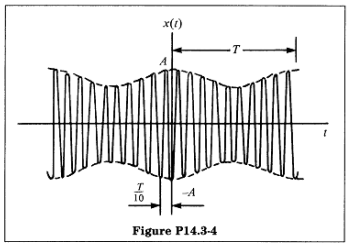

Figure P14.3-4

(e)

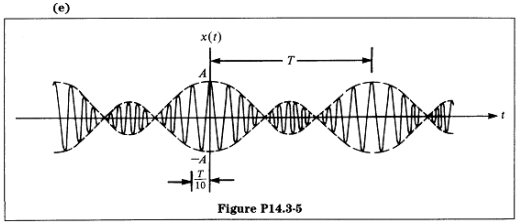

Figure P14.3-5

(f)

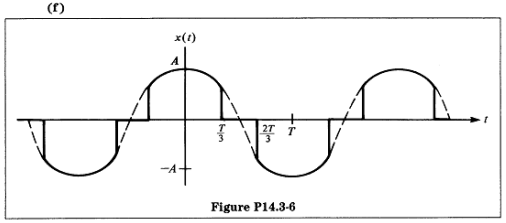

Figure P14.3-6

(a) ii

(b) i

(c) iii

(d) vi

(e) v

(f) iv

(i)

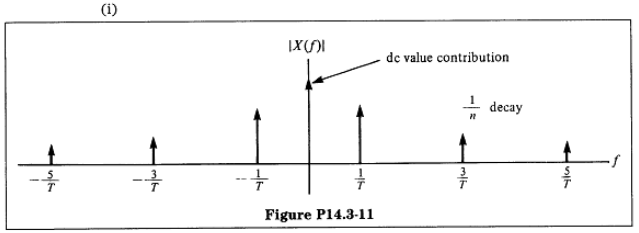

Figure P14.3-11

(ii)

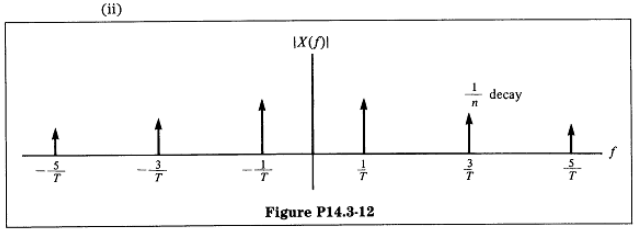

Figure P14.3-12

(iii)

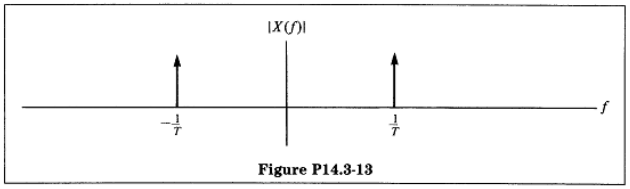

Figure P14.3-13

(iv)

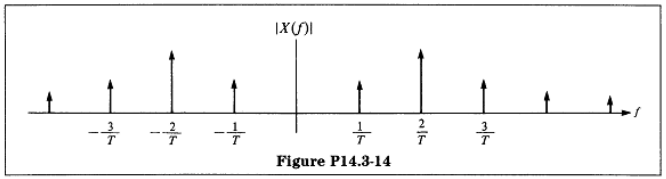

Figure P14.3-14

(v)

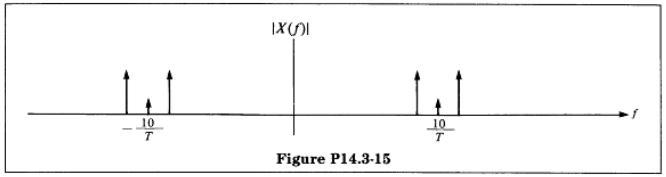

Figure P14.3-15

(vi)

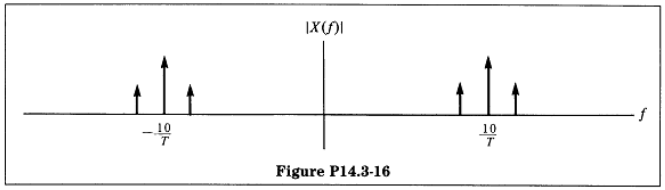

Figure P14.3-16

8.22. In Figure P8.22(a), a system is shown with input signal $x(t)$ and output signal $y(t)$ The input signal has the Fourier transform $X(j\omega)$ shown in Figure P8.22(b). Determine and sketch $Y(j\omega)$, the spectrum of $y(t)$.

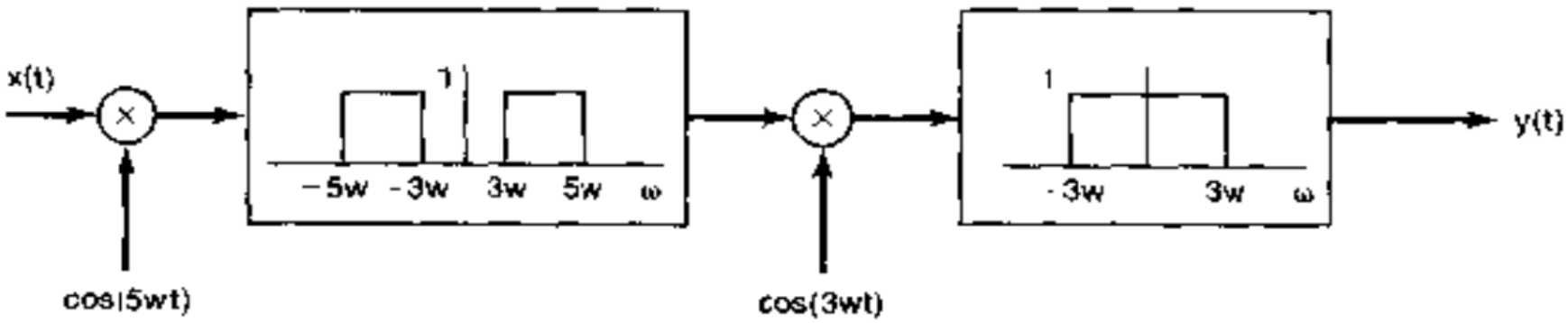

(a)

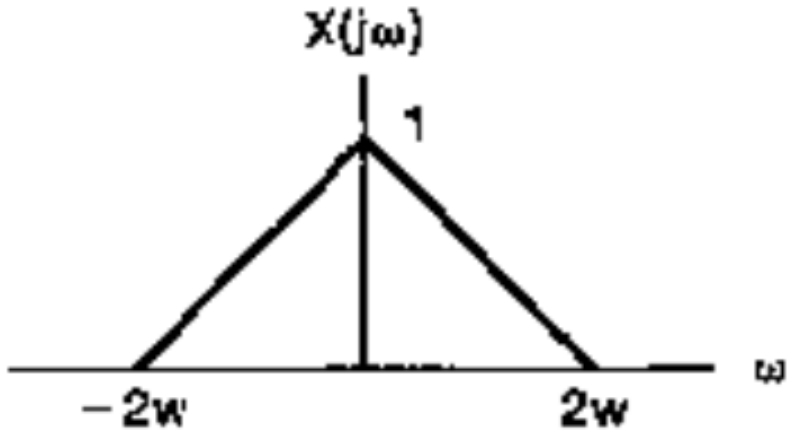

(b)

Figure P8.22 *Continued*

8.22. Sketches for (i) the Fourier transforms for each of the intermediate outputs and (ii) the Fourier transform $Y(j\omega)$ of $y(t)$ are shown in Figure S8.22.

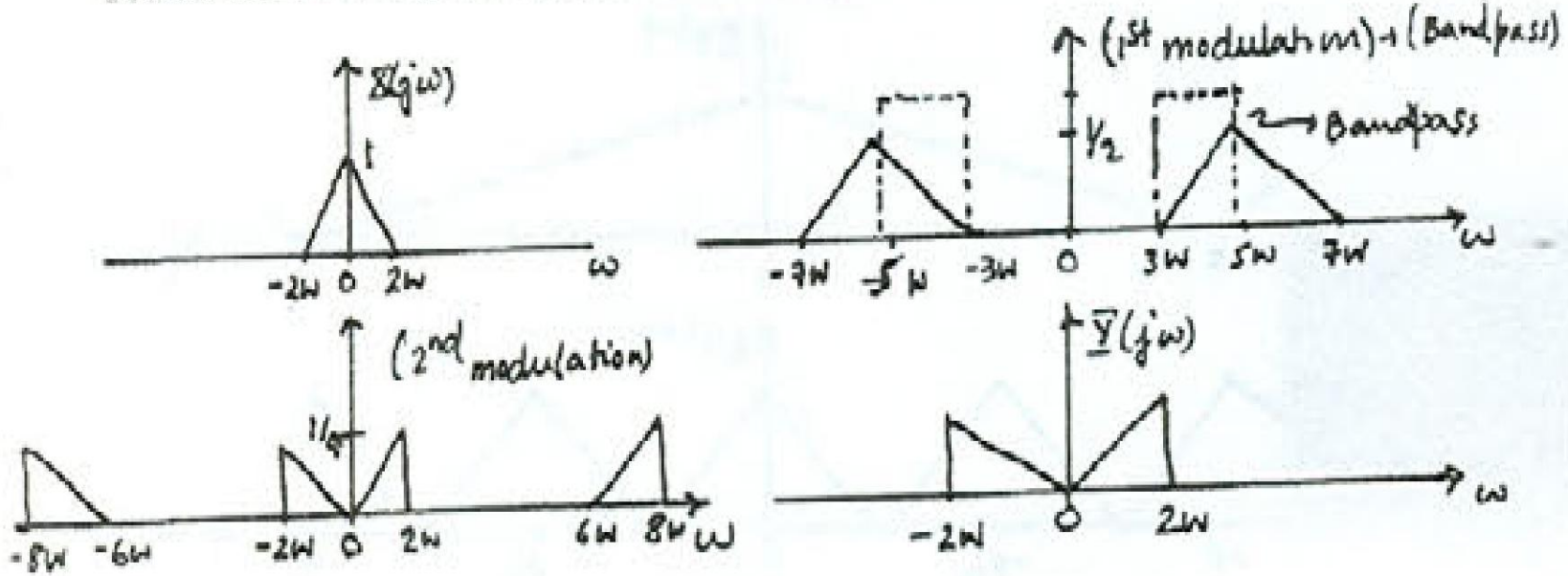

8.23. In Section 8.2, we discussed the effect of a loss of synchronization in phase between the carrier signals in the modulator and demodulator in sinusoidal amplitude modulation. We showed that the output of the demodulation is attenuated by the cosine of the phase difference, and in particular, when the modulator and demodulator have a phase difference of $\pi/2$, the demodulator output is zero. As we demonstrate in this problem, it is also important to have *frequency* synchronization between the modulator and demodulator.

Consider the amplitude modulation and demodulation systems in Figure 8.8 with $\theta_c = 0$ and with a change in the *frequency* of the demodulator carrier so that

$$w(t) = y(t)\cos\omega_d t,$$

where

$$y(t) = x(t)\cos\omega_c t.$$

Let us denote the difference in frequency between the modulator and demodulator as $\Delta\omega$ (i.e., $\omega_d - \omega_c = \Delta\omega$). Also, assume that $x(t)$ is band limited with $X(j\omega) = 0$ for $|\omega| \geq \omega_M$, and assume that the cutoff frequency ω_{co} of the lowpass filter in the demodulator satisfies the inequality

$$\omega_M + \Delta\omega < \omega_{co} < 2\omega_c + \Delta\omega - \omega_M.$$

(a) Show that the output of the lowpass filter in the demodulator is proportional to $x(t)\cos(\Delta\omega t)$.

(b) If the spectrum of $x(t)$ is that shown in Figure P8.23, sketch the spectrum of the output of the demodulator.

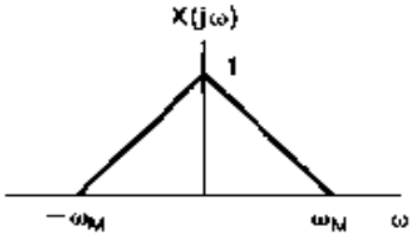

Figure P8.23

8.23. (a) We have

$$w(t) = x(t)\cos(\omega_c t)\cos(\omega_d t).$$

Using Trigonometric identities, we have

$$\begin{aligned} w(t) &= \frac{1}{2}x(t)\left\{\cos[(\omega_c+\omega_d)t] + \cos[(\omega_c-\omega_d)t]\right\} \\ &= \frac{1}{2}x(t)\left\{\cos[(\omega_c+\omega_d)t] + \cos[\Delta\omega t]\right\} \end{aligned}$$

Now, $\frac{1}{2}x(t)\cos[(\omega_c+\omega_d)t]$ has a spectrum in the range $\omega_c+\omega_d-\omega_M \le |\omega| \le \omega_c+\omega_d+\omega_M$. This range may also be expressed as $2\omega_c + \Delta\omega - \omega_M \le |\omega| \le 2\omega_c + \Delta\omega + \omega_M$ Since, we are given that $W < 2\omega_c + \Delta\omega - \omega_M$, lowpass filtering will result in the output $\frac{1}{2}x(t)\cos(\Delta\omega t)$.

(b) We sketch the spectrum of the output for $\Delta\omega = \omega_M/2$ in Figure S8.23.

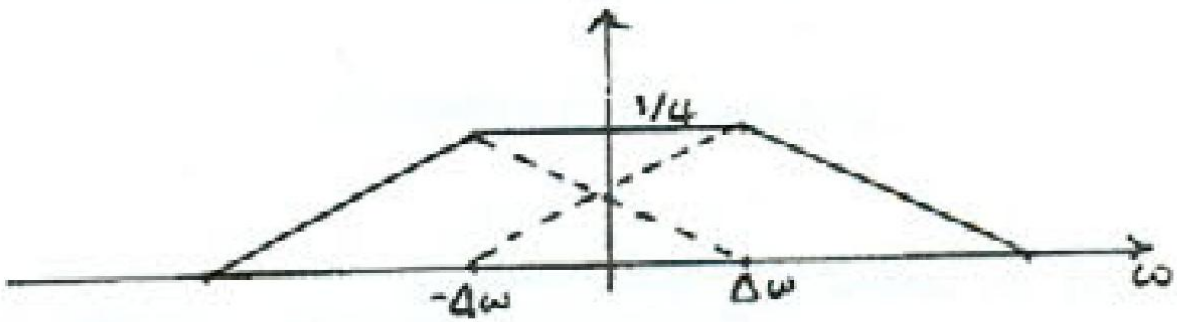

Figure S8.23

8.32. Consider a discrete-time signal $x[n]$ with Fourier transform shown in Figure P8.32(a). The signal is amplitude modulated by a sinusoidal sequence, as indicated in Figure P8.32(b).

(a) Determine and sketch $Y(e^{j\omega})$, the Fourier transform of $y[n]$.

(b) A proposed demodulation system is shown in Figure P8.32(c). For what value of θ_c, ω_{lp}, and G will $\hat{x}[n] = x[n]$? Are any restrictions on ω_c and ω_{lp} necessary to guarantee that $x[n]$ is recoverable from $y[n]$?

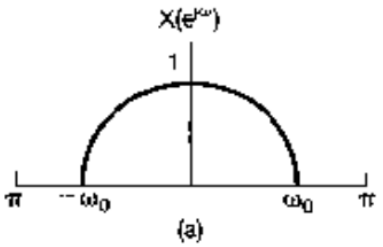

(a)

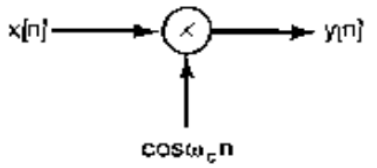

(b)

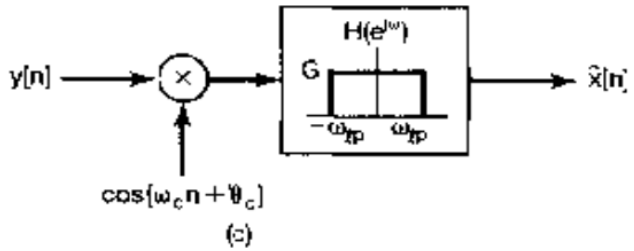

(c)

Figure P8.32

8.32. (a) Let $c[n] = \cos(\omega_c n)$. Noting that $y[n] = x[n]c[n]$, we have

$$Y(e^{j\omega}) = \frac{1}{2\pi}\int_{-\pi}^{\pi} C(e^{j\theta})X(e^{j(\omega-\theta)})d\theta.$$

We now have

$$C(e^{j\omega}) = \pi\sum_{k=-\infty}^{\infty}[\delta(\omega-\omega_c+2k\pi)+\delta(\omega+\omega_c+2k\pi)].$$

Therefore, $Y(e^{j\omega})$ is

$$Y(e^{j\omega}) = \frac{1}{2}\left[X(e^{j(\omega-\omega_c)})+X(e^{j(\omega+\omega_c)})\right].$$

If we assume that $\omega_c > \omega_{lp}$ and $\omega_c < \pi - \omega_{lp}$, then $Y(e^{j\omega})$ may be sketched as shown in Figure S8.32.

(b) Let $c_1[n] = \cos(\omega_c n + \theta_c)$. Let $q[n] = y[n]c_1[n]$. Then,

$$Q(e^{j\omega}) = \frac{1}{2\pi}\int_{-\pi}^{\pi} C_1(e^{j\theta})Y(e^{j(\omega-\theta)})d\theta.$$

(b) Let $c_1[n] = \cos(\omega_c n + \theta_c)$. Let $q[n] = y[n]c_1[n]$. Then,

$$Q(e^{j\omega}) = \frac{1}{2\pi}\int_{-\pi}^{\pi} C_1(e^{j\theta})Y(e^{j(\omega-\theta)})d\theta.$$

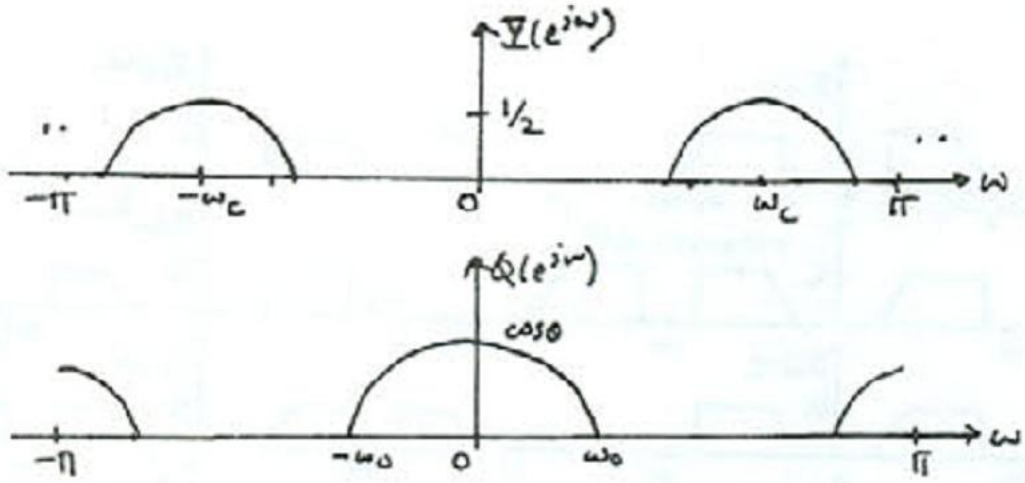

Figure S8.32

We now have

$$C_1(e^{j\omega}) = \pi\sum_{k=-\infty}^{\infty}\left[e^{j\theta_c}\delta(\omega-\omega_c+2k\pi) + e^{-j\theta_c}\delta(\omega+\omega_c+2k\pi)\right].$$

Therefore, $Q(e^{j\omega})$ is

$$Q(e^{j\omega}) = \frac{1}{2}\left[e^{j\theta_c}Y(e^{j(\omega-\omega_c)}) + e^{-j\theta_c}Y(e^{j(\omega+\omega_c)})\right].$$

This is as shown in Figure S8.32.

Thus, $\hat{x}[n] = x[n]$ if $G = 1/\cos(\theta_c)$. We definitely require that $\cos(\theta_c) \neq 0$. This implies that θ_c should not be an odd multiple of $\pi/2$. The restrictions to ω_c and ω_{lp} are the same as the ones mentioned in part (a). That is, $\omega_c > \omega_{lp}$ and $\omega_c < \pi - \omega_{lp}$.